Online ISSN: 2682-2628
Print ISSN: 2682-261X

IJCBR

International Journal of Cancer and Biomedical Research

https://jcbr.journals.ekb.eg

Tramadol and/or ketamine repurposing as potential anticancer drugs in metastatic castration-resistant prostate cancer cell lines

Neveen A. Hussein, Mohammad A. Ahmad and Khaled S. Ali

PUBLISHED BY
EACR EGYPTIAN ASSOCIAN FOR CANCER RESEARCH
Since 2014

INTERNATIONAL JOURNAL OF CANCER AND BIOMEDICAL RESEARCH (IJCBR)

RESEARCH ARTICLE

Tramadol and/or Ketamine Repurposing as Potential Anticancer Drugs in Metastatic Castration-Resistant Prostate Cancer Cell Lines

Neveen A. Hussein[1], Mohammad A. Ahmad[2] and Khaled S. Ali[1]

[1] *Applied Medical Chemistry Department, Medical Research Institute, Alexandria University, Egypt*
[2] *Clinical Pathology Department, Military Medical Academy, Cairo, Egypt*

ABSTRACT

Prostate cancer (PCa) progression to androgen independence is the main cause of death. Although all metastatic patients initially responded to anti-androgen therapy, most of them failed hormonal treatments in less than 2 years. Tramadol is an opioid agonist with the central effect of treating pain. Ketamine is a flexible medication that has a wide range of clinical uses. This *in vitro* study evaluated the repurposing of tramadol and/or ketamine as potential anticancer drugs. Moreover, the impact of these drugs on cell death pathways was assessed. PC-3 and DU145 cell lines were treated with tramadol and/or ketamine. Apoptosis, autophagy, necroptosis, parthanatos, endoplasmic reticulum stress, the Raf/MEK/ERK pathway, and epithelial-mesenchymal transition-related genes were determined by real-time PCR. Current data showed upregulation of most gene expression in PC-3 cells treated with TRA and/or KET compared to untreated cancer cells, except for N-cadherin, which was insignificantly downregulated by KET. On the other hand, gene expressions in DU145 showed an insignificant difference in all treated cells compared to each other or untreated cancer cells, except for significant up-regulation of ATG3, Beclin1, and ATF6 by KET (P = 0.047, 0.035, and 0.042, respectively), IRE1 by TRA (P = 0.023) and N-cadherin by the combined drug (P = 0.014) compared to untreated cells. PC-3 cells were significantly more susceptible to tramadol and/or ketamine than DU145 cells. ROS-induced cell death pathways could be the mechanism by which tramadol and ketamine exert their anticancer effects against metastatic PCa. Targeting cell death pathways is an ideal strategy for developing new anticancer therapies**.**

Keywords: Metastatic castration-resistant PCa; PC-3; DU145; Tramadol; Ketamine

Editor-in-Chief: Prof. M.L. Salem, PhD - Article DOI: 10.21608/JCBR.2024.255088.1327

ARTICLE INFO

Article history
Received: December12, 2023
Revised: January 18, 2024
Accepted: February 28, 2024

Correspondence to
Neveen A. Hussein,
Medical Research Institute,
Alexandria University,
Alexandria, Egypt
Tel.: 01223667426, Fax: 03-4283789.
Email: neveen.hussien@alexu.edu.eg
ORCID: 0000-0001-9889-8063

INTRODUCTION

Prostate cancer (PCa) is the fourth most common cancer diagnosed in the world (7.3%, >1,400,000 yearly) and the eighth cause of cancer deaths (3.8 %, > 375 000). PCa is the second most common cancer in men (14.1%) and the fifth cause of cancer death (6.8%) in 2020 (Sung et al., 2021). Despite progress in PCa therapy, most patients eventually reach the metastatic castration-resistant stage with significant morbidity and minimal survival benefit (13-32 months) (Gillessen et al., 2020). This aggressive stage of PCa is still incurable; therefore, effort must be made urgently to explore more effective treatments.

Tramadol is an opioid agonist with a central effect to treat moderate to severe pain. Tramadol is effective for postoperative, neuropathic, and lower back pains, as well as pain linked with fibromyalgia, osteoarthritis, and cancer (Barakat, 2019). The activation of μ-opioid receptor and the inhibition of reuptake of monoamines (norepinephrine and serotonin) released from the nerve end was identified as a mechanism of tramadol's action. Opioid receptors are expressed more strongly in numerous solid human cancers. In PCa the expression of κ-opioid receptor was increased (Lec et al., 2020).

Ketamine is a flexible medication that has a wide range of clinical uses either alone or in combination with other medications. Ketamine's mechanism of antagonistic action on N-methyl-D-aspartate (NMDA) receptor is thought to be the primary source of its therapeutic benefits. Ketamine is a drug of high quality in cases where depression, opioid tolerance, pains (neuropathic, inflammatory), or a combination of these factors are problematic. The effectiveness of cancer pain management may be increased by combining ketamine and opioids (Abdollahpour et al., 2020).

Based on signal dependence, cell death entities are divided into programmed cell death (PCD) or non-PCD (necrosis). PCD can also be categorized as apoptotic cell death (anoikis, apoptosis) or non-apoptotic cell death containing mitochondrial-dependent cell death (parthanatos, mitoptosis), vacuole presenting cell death (autophagy, methuosis, paraptosis, entosis,), immune-reactive cell death (NETosis, pyroptosis), iron-dependent cell death (ferroptosis), as well as necroptosis (Yan et al., 2020).

Death receptors (DRs) such as Fas cell surface death receptor and TNF receptor superfamily member 1A, 10A (TNFRSF10A, TRAILR1 or DR4), and 10B are primarily responsible for extrinsic apoptosis. A multiprotein complex known as the death-inducing signaling complex, which is normally assembled at the receptor's intracellular domain because of DR ligation, serves as a molecular platform to control the activities of caspases (Dickens et al., 2012).

Autophagy, a catabolic process, eliminates defective and damaged cellular components via lysosomes. Autophagy-related genes (ATG) control the process of autophagy. In the ATG8 conjugation system, ATG3 acts as an E2 ubiquitin-like conjugating enzyme that aids in phagophore elongation. Beclin1, a key regulator of autophagy, recruits various proteins necessary for both maturation as well as elongation of the autophagosome (Hasan et al., 2022).

Necroptosis is the most well-known type of programmed necrosis, with characteristics of both apoptosis and necrosis. Receptor-interacting protein kinases (RIPKs) are recruited to macromolecular complexes by a variety of cell surface receptors, including DRs, Toll-like receptors, and T-cell receptors. The essential elements of the necrosome are RIPK1 and RIPK3. RIPK3 phosphorylates the downstream mixed lineage kinase domain-like protein (MLKL), which causes MLKL to oligomerize and go to the plasma membrane where it causes cell death (Mohanty et al., 2022). Parthanatos is a type of cell death caused by poly (ADP-ribose) polymerase 1 (PARP1), that results from DNA damage. PARP1 is an abundant nuclear protein that serves as a DNA nick-sensing enzyme (Huang et al., 2022).

Endoplasmic reticulum stress (ERS) is mostly caused by apoptosis, but other forms of cell death, such as necrosis, necroptosis, or dysregulated autophagy, have also been implicated. Three transmembrane receptors [protein kinase RNA-like ER kinase (PERK), inositol-requiring enzyme 1 (IRE1), and activating transcription factor 6 (ATF6)] are used to identify unfolded/misfolded proteins. The transcription of genes that affect protein folding/capacity, autophagy, and apoptosis is controlled by the activation of unfolding protein response (UPR) through ERS pathways (Hetz et al., 2020). In a variety of cell types, the UPR is involved in interplay with the epithelial-mesenchymal transition (EMT). Under conditions of extreme hypoxia or persistent ERS, the UPR improves EMT in gastric cancer cells and causes irreversible EMT in human peritoneal mesothelial cells (Shen et al., 2015).

Consequently, this *in vitro* study aimed to evaluate the repurposing of tramadol and/or ketamine as potential anticancer medications and their impact on the regulation of cell death pathways in metastatic castration-resistant PCa cell lines.

MATERIAL AND METHODS

Cell culture

Two androgen-independent PCa cell lines PC-3 (RRID: CVCL-0035, CRL-1435) and DU145 (RRID: CVCL-0105, HTB-81) and normal human gingival fibroblast cells (HGF) (American Type Culture Collection, USA) were cultured at 37°C in Dulbecco's modified Eagle medium (Gibco, Carlsbad, CA, USA) containing 4.5 g/L glucose,

0.2 mmol/mL L-glutamine, 10% fetal bovine serum, 50 U/mL penicillin, 50 mg/mL streptomycin in a humidified atmosphere contained 5% CO_2.

Tramadol

Fifteen tablets of tramadol (225 mg/tablet) were finely powdered. Three g of TRA powder were mixed with 60 mL methanol and then filtered. The residue was washed twice with 10 ml of methanol and then the washings were added to the filtrate and diluted with methanol to 100 ml. Aliquots of the tablet solution were diluted with methanol to 0.1 M in 100 ml solution (Belal et al., 2009). For cell lines treatment, this solution was evaporated to dryness and then redissolved in 100 ml of distilled water to produce 0.1 M TRA solution. Gas chromatography-mass spectrometry was used to characterize TRA (Supplementary Figure 1).

ketamine

To obtain 30 mM KET stock solution, 16.4 ml of KET solution (50 mg / mL, Rotexmedica, Germany) was added to 83.6 mL of distilled water.

Cell cytotoxicity

PC-3 and DU145 (approximately $1x10^5$) were seeded in 96-well plates. After 24 h of incubation, TRA and/or KET were added with different concentrations in both cells: TRA (0.8, 1.6, 3.2, 6.4, 12.8, 14.5 mM), KET (1.3, 1.9, 2, 2.5, 3.1 mM), TRA+KET (0.1+0.1, 0.2+0.2, 0.4+0.4, 0.8+0.8, 1.6+1.6, 3.2+3.2 mM); while for HGF normal cell line: TRA (3.2, 6.4, 12.8, 14.5, 19.2, 28.8 mM), KET (0.1, 0.7, 1.3, 2.5, 3 mM), TRA+KET (1.6+1.6, 3.2+3.2, 6.4+6.4 mM). Phosphate buffered saline was added to control cancer cells. After 48 h incubation, cell cytotoxicity was assessed using 5 mg/mL MTT solution. The absorbance at 570 nm was measured. The experiments were repeated three times.

The MTT data of TRA and/or KAT was analyzed to determine IC_{50} values of TRA and/or KET in normal and cancer cell lines. Moreover, CompuSyn software (https://www.combosyn.com/) determined the combination index (CI) [CI=1 indicates an additive effect, CI<1 synergism and CI>1 antagonism in the drug combination], as well as dose reduction index (DRI) [DRI=1 indicates no dose reduction, while DRI<1 and DRI>1indicates unfavorable and favorable dose-reduction respectively in drug combination compared to monotherapy]. Selectivity index (SI) was estimated from the ratio of IC_{50} of drugs in normal cell line to that in cancer cell lines.

Genes profiling

The profile of TNFRSF10A, ATG3, Beclin1, RIPK1, PARP1, IRE1, ATF6, Raf1, MEK2, ERK1, and E-, N-cadherin expressions was established in PC-3 and DU145 cells, where $1x10^6$ cells from each cell line were seeded in 100 mm plates and incubated overnight. PC-3 cells were treated with 1.0 mM TRA, 1.0 mM KET, and combined drug (1.0 TRA+1.0 KET mM), while DU145 was treated with 0.3 mM TRA, 0.3 mM KET, and combined drug (0.3 TRA+0.3 KET mM). After 48 h of TRA and/or KAT treatment, total RNA was extracted using the RNeasy Mini Kit (Qiagen, Germany) from all treated and untreated cancer cell pellets. The purity and concentration in each sample were measured using a NanoDrop spectrometer (Thermo Fisher Scientific). cDNA was synthesized using the QuaniTect Reverse Transcription Kit (Qiagen). Finally, quantitative PCR was performed using Maxima SYBR Green qPCR Master Mix (Thermo Fisher) and StepOne Plus Real-Time PCR instrument. GAPDH was used as a housekeeping gene. The gene expressions were expressed using $2^{-\Delta\Delta Ct}$. Primer sequences (Invitrogen, Thermo Fisher) were listed in Table 1.

Statistical analyses

Data were analyzed using IBM SPSS software package version 20.0. One-way ANOVA test, a Pairwise comparison between each two groups was done using Post Hoc Test (Bonferroni). Student t-test was applied for comparison between PC-3 and DU145. $P<0.05$ was statistically significant.

RESULTS

IC_{50} values, selectivity index, combination index

By increasing the concentrations of TRA and/or KET in HGF, PC-3, and DU145, the cell viability % was decreased. IC_{50} values in HGF, PC-3, and DU145 cell lines were 10.25, 4.50, and 3.54

respectively for TRA, 2.80, 1.74, and 1.42 respectively for KET, while 5.12, 3.0, and 0.85 respectively for combined drug (Figure 1). The SI in PC-3 and DU145 for TRA was 2.27, 2.90 respectively, for KET was 1.61, 2.26 respectively, for the combined drug was 1.71, 6.02 respectively. The SI values of each drug in both cell lines were greater than 1, indicating their selectivity against PC-3 and DU145 cancer cell lines.

The mean CI value of the combined drug (TRA + KET) in PC-3 was 0.617 $\pm$ 0.404 indicating the synergistic effect of the combined therapy in PC-3 cell line where strong synergism at 0.1, 0.2 mM doses, synergism at 0.4, 0.8 mM doses, and nearly additive at high doses of 1.6 and 3.2 mM. The mean CI value of the combined drug in DU145 was 0.605 $\pm$ 0.321 indicating the synergistic effect of combined therapy in DU145 cell line where strong synergism at 0.1, 0.2 mM doses, synergism at 0.4 mM dose, moderate synergism at 0.8, 3.2 mM doses and nearly additive at1.6 mM (Tables 2, 3 and Figure 2).

Table 1. Primer sequences.

Genes	Primer sequences
TNFRSF10A	F: GTGTGGGTTACACCAATGCTTCC
	R: CCTGGTTTGCACTGACATGCTG
ATG3	F: ACTGATGCTGGCGGTGAAGATG
	R: GTGCTCAACTGTTAAAGGCTGCC
Beclin1	F: CTGGACACTCAGCTCAACGTCA
	R: CTCTAGTGCCAGCTCCTTTAGC
RIPK1	F: TATCCCAGTGCCTGAGACCAAC
	R: GTAGGCTCCAATCTGAATGCCAG
PARP1	F: CCAAGCCAGTTCAGGACCTCAT
	R: GGATCTGCCTTTTGCTCAGCTTC
IRE1	F: CCGAACGTGATCCGCTACTTCT
	R: CGCAAAGTCCTTCTGCTCCACA
ATF6	F: CAGACAGTACCAACGCTTATGCC
	R: GCAGAACTCCAGGTGCTTGAAG
Raf1	F: TCAGGAATGAGGTGGCTGTTCTG
	R: CTCGCACCACTGGGTCACAATT
MEK2	F: GTGGTCACCAAAGTCCAGCACA
	R: CACGATGTACGGCGAGTTGCAT
ERK1	F: TGGCAAGCACTACCTGGATCAG
	R: GCAGAGACTGTAGGTAGTTTCGG
E-cadherin	F: GCCTCCTGAAAAGAGAGTGGAAG
	R: TGGCAGTGTCTCTCCAAATCCG
N-cadherin	F: CCTCCAGAGTTTACTGCCATGAC
	R: GTAGGATCTCCGCCACTGATTC
GAPDH	F: GTCTCCTCTGACTTCAACAGCG
	R: ACCACCCTGTTGCTGTAGCCAA

Gene expressions

For PC-3 cell lines: significant up-regulation of TNFRSF10A, ATG3, Beclin1, RIPK1, PARP1, Raf1, and MEK2 expression was detected in TRA, KET, and combined-treated cell lines compared to untreated cancer cells. The expression of ERK1, IRE1, ATF6, E, and N-cadherin was up-regulated in all treated cells compared to untreated cells, except that N-cadherin was insignificantly down-regulated in KET-treated cells. Significant elevation in ERK1, IRE1 expression by TRA alone ($P<0.001$) or combined ($P=0.019$) and ATF6, N-cadherin expression in TRA-treated cells ($P<0.001$, 0.004 respectively) was observed. Expression of all genes was down-regulated in KET, as well as combined-treated cells compared to TRA-treated cells. On the other hand, insignificant upregulation of all gene expressions in combined-treated cells compared to KET-treated cells, except E-cadherin which was insignificantly downregulated.

For DU145 cell lines: the expression of all studied genes showed an insignificant difference in all treated cells compared to each other or untreated cells ($P>0.05$), except significant up-regulation of ATG3, Beclin1, ATF6 by KET ($P=0.047$, 0.035, 0.042 respectively), IRE1 by TRA ($P=0.023$) and N-cadherin by combined drug ($P=0.014$) compared to untreated cancer cells (Figure 3). There was a significant difference between PC-3 and DU145 for all studied genes ($P<0.05$) except ATF6 ($P=0.221$).

DISCUSSION

According to this study, PC-3 and DU145 cell lines respond to TRA and KET differently. Compared to untreated cancer cells, TRA and/or KET upregulate the expression of apoptosis (TNFRSF10A), autophagy (ATG3, Beclin1), necroptosis (RIPK1), parthanatos (PARP1), endoplasmic reticulum stress (IRE1, ATF6), Raf/MEK/ERK pathway and epithelial-mesenchymal transition (E-, N-cadherin)-related genes in PC-3 cells. Earlier research suggested that TRA administration significantly reduced the activity of the mitochondrial electron transport chain complexes I, III, and IV, which enhanced ROS generation and oxidative stress (Mohamed and Mahmoud, 2019).

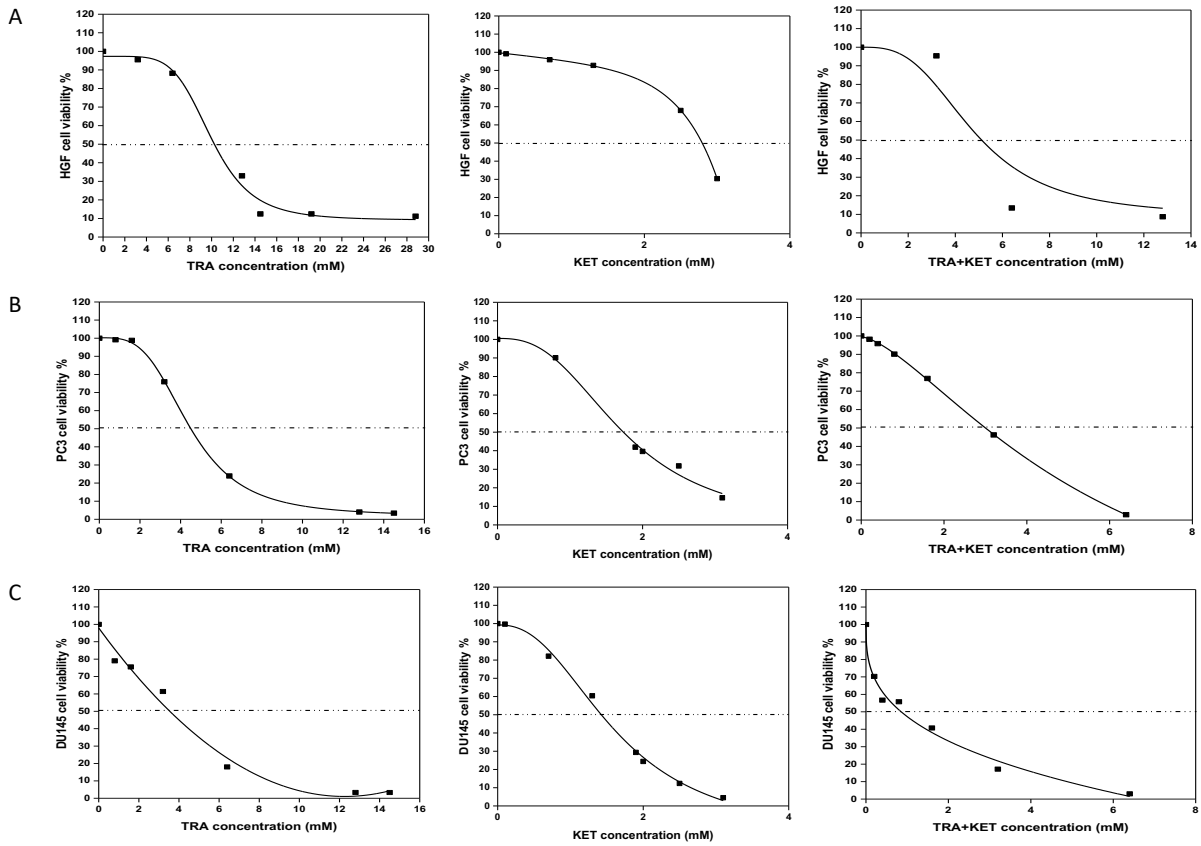

Figure 1. Cell viability % of (A) HGF, (B) PC-3, and (C) DU145 cell lines with different concentration of TRA and/or KET drugs.

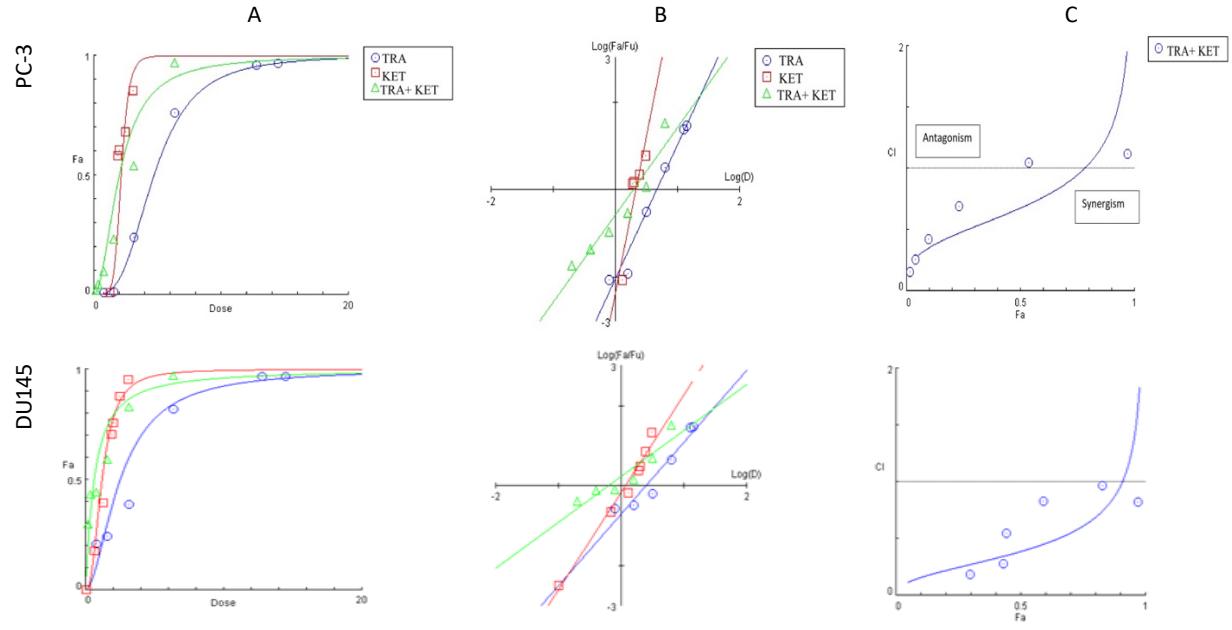

Figure 2. (A) Dose-effect curves, (B) median-effect plots, (C) combination index plots of TRA and/or KET in PC-3 and DU145 cell lines.

Table 2. Fa, IC_{50}, CI, and DRI of TRA (mM) and/or KET (mM) in PC-3.

Compound			Fa	Parameters			CI	DRI
TRA		KET		m	Dm	R		[TRA; KET]
D_1								
0.8			0.009	3.059	4.738	0.987		
1.6			0.012					
3.2			0.241					
6.4			0.761					
12.8			0.960					
14.5			0.966					
		D_2						
		1.3	0.009	7.127	2.159	0.910		
		1.9	0.581					
		2.0	0.604					
		2.5	0.682					
		3.1	0.854					
0.1	+	0.1	0.018	1.994	2.007	0.956	0.159	[12.835;12.329]
0.2	+	0.2	0.042		(1.00+1.00)		0.261	[8.545; 6.970]
0.4	+	0.4	0.099				0.427	[5.747; 3.958]
0.8	+	0.8	0.231				0.689	[3.999; 2.280]
1.6	+	1.6	0.538				1.046	[3.114; 1.379]
3.2	+	3.2	0.971				1.119	[4.669; 1.105]
			Simulation					
			0.5				0.677	[4.720; 2.151]
			0.75				0.948	[3.896; 1.446]
			0.9				1.339	[3.216; 0.973]
			0.95				1.701	[2.822; 0.742]

Table 3. Fa, IC_{50}, CI, and DRI of TRA (mM) and/or KET (mM) in DU145.

Compound			Fa	Parameters			CI	DRI
TRA		KET		m	Dm	R		[TRA; KET]
D_1								
0.8			0.210	1.803	2.511	0.963		
1.6			0.245					
3.2			0.386					
6.4			0.820					
12.8			0.967					
14.5			0.967					
		D_2						
		0.1	0.003	2.432	1.197	0.988		
		0.7	0.179					
		1.3	0.396					
		1.9	0.707					
		2.0	0.756					
		2.5	0.877					
		3.1	0.955					
0.1	+	0.1	0.297	1.148	0.626	0.929	0.183	[15.573; 8.401]
0.2	+	0.2	0.433		(0.313+0.313)		0.279	[10.817; 5.360]
0.4	+	0.4	0.443				0.548	[5.524; 2.722]
0.8	+	0.8	0.593				0.831	[3.866; 1.747]
1.6	+	1.6	0.829				0.965	[3.760; 1.430]
3.2	+	3.2	0.970				0.823	[5.418; 1.567]
			Simulation					
			0.5				0.386	[8.017; 3.823]
			0.75				0.610	[5.666; 2.308]
			0.9				0.968	[4.004; 1.393]
			0.95				1.328	[3.162; 0.988]

Fa: fractional affected; m: slope, signifies shape; Dm: IC_{50}, signifies potency; r: linear correlation coefficient, signifies conformity; CI: combination index; DRI: dose-reduction index.

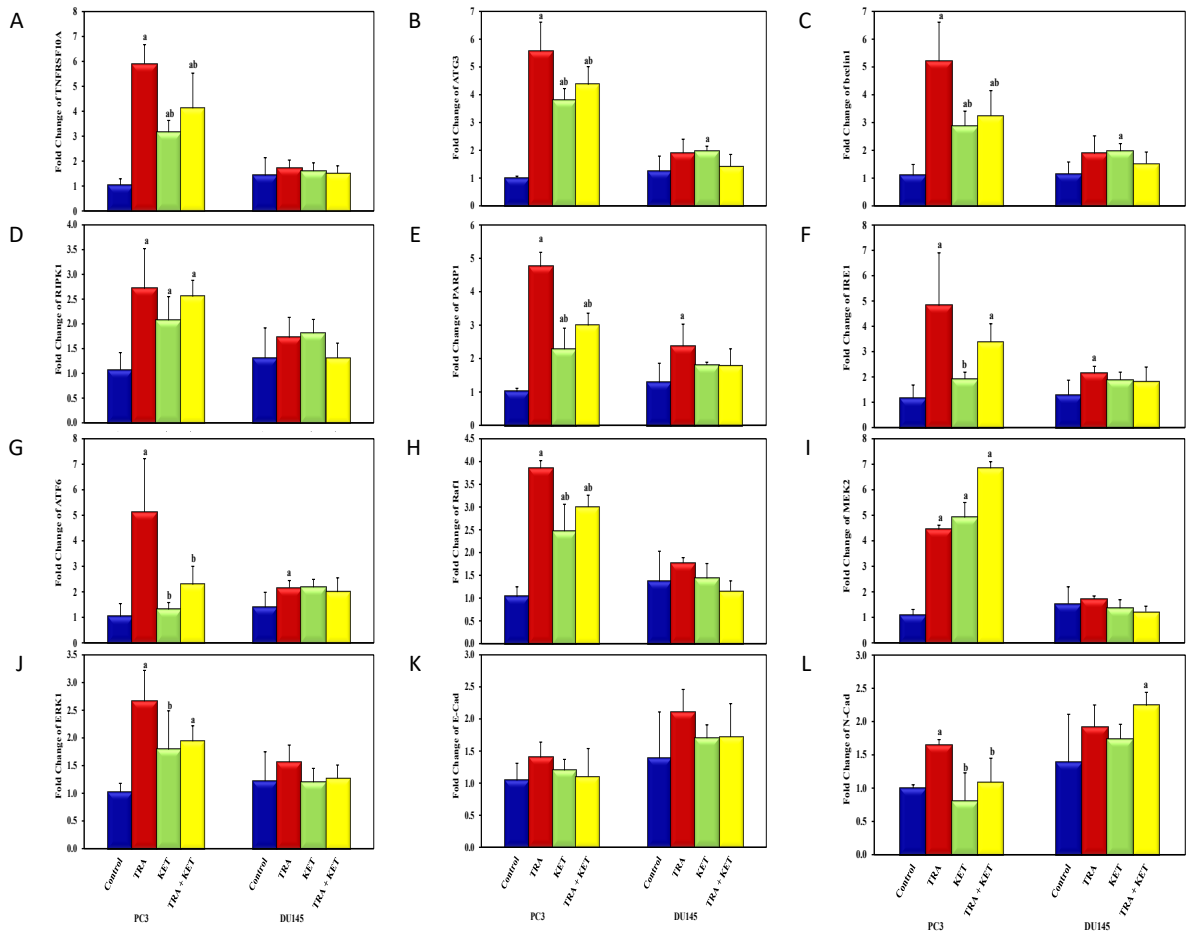

Figure 3. Relative expression of (A) TNFRSF10A, (B) ATG3, (C) Beclin1, (D) RIPK1, (E) PARP1, (F) IRE1, (G) ATF6, (H) Raf1, (I) MEK2, (J) ERK1, (K) E-Cadherin, and (L) N-Cadherin genes in PC-3 and DU145 human prostate Cells. a: significant with control, b: significant with TRA, and c: significant with KET.

In addition, a single intravenous dose of TRA (25 mg/kg) significantly increased mitochondrial ROS, lipid peroxidation, and protein carbonyl, while lowering glutathione. These findings revealed that macromolecule damage, mitochondrial malfunction, and cell death are linked to TRA-induced oxidative stress (Bameri et al., 2018). ROS can cause inflammation by activating the redox-sensitive transcription factor NF-κB, which then triggers the transcription of other inflammatory mediators and cytokines. Moreover, TRA increases the expression of inducible nitric oxide synthase (iNOS) gene and protein level (Mohamed and Mahmoud, 2019). During oxidative stress, NO can interact with superoxide radicals to generate peroxynitrite, which damages macromolecules. Combining oxidative stress and inflammation can elicit apoptosis, which causes cell death (Mahmoud et al., 2017).

According to Ito et al. (2015), KET can cause the mitochondrial oxidative phosphorylation system malfunction by inhibiting the activity of complexes I and V. This leads to lower ATP generation, decreased NADH oxidation, an elevated NADH / NAD^+ ratio, and enhanced mitochondrial fission. Furthermore, KET resulted in mitochondrial deterioration and ROS production (Ito et al., 2015).

TP53, AP-1, or NF-κB (Mendoza et al., 2008) transcriptional factors are usually responsible for upregulating TNFRSF10A at the transcriptional level (Li et al., 2015). Both TRA and KET raise NF-κB level, which in turn upregulate the expression of TNFRSF10A at the transcriptional level, suggesting that both drugs may trigger the extrinsic apoptotic pathway by upregulating TNFRSF10A.

Increased level of ROS can control autophagy via several pathways, including activation of unc-51 like autophagy activating kinase 1 (ULK1)

complex and AMP-activating protein kinase (AMPK) signaling, interruption of Bcl2/Beclin1 interaction, oxidation of ATG4, reduces the activity of mTORC1 and changes the homeostasis of mitochondrial that triggers mitophagy. ROS-activated NF-κB causes an increase in the autophagy gene (p62, Beclin1) (Redza-Dutordoir and Averill-Bates, 2021).

Beclin1 from anti-apoptotic protein B-cell lymphoma 2, can be activated by oxidative stress to create Beclin1-Vps34-ATG14 complex, which results in membrane separation and autophagy nucleation, initiating autophagy pathway (Valente et al., 2014). Degradation of catalase by autophagy causes mitochondrial ROS buildup, macromolecule damage, and cell death. ATP level was also increased during autophagy, exposing intracellular phosphatidylserine, and causing it to emit apoptotic signals (Ito et al., 2005).

Apoptosis and necroptosis occur concurrently, whereas necroptosis subsequently dominates. The increase of mitochondrial ROS and changes in mitochondrial membrane permeability are necessary for the transition from apoptosis to necroptosis, where ROS acts as a driving force for both pathways (Beretta and Zaffaroni, 2022). RIPK1 / RIPK3 activation improves the anti-tumor response by circulating cytokines/chemokines in the cancer microenvironment and intensifies the necroptotic death signal to inhibit metastasis by boosting ROS deposition (Zhang et al., 2017).

Even though PARP1 is essential for preserving genomic stability by promoting DNA repair, prolonged ROS/RNS-induced severe DNA damage causes PARP1 to be recruited and activated. PARP1 overactivation produces free poly (ADP-ribose) that acts as a death signal from the nucleus to mitochondria, causing the release of apoptosis-inducing factor (AIF), which is translocated with macrophage migration inhibitory factor to the nucleus and accelerates ATP and NAD^+ decline, resulting in organ dysfunctions, DNA fragmentation, and necrosis (Huang et al., 2022). Apoptosis can also be induced by the released AIF via caspase-dependent and independent mechanisms (Pazzaglia and Pioli, 2019). In ROS-dependent cell death, intracellular Ca^{2+} and PARP1 hyperactivation are interdependent. The activation of PARP1 is influenced by increases in $[Ca^{2+}]i$ that is needed as a cofactor. Furthermore, PARP1 activation can act reciprocally to increase $[Ca^{2+}]i$. Even in the absence of DNA strand breaks, Ca^{2+} can hyperactivate PARP1 (Zhang et al., 2014).

The unfolding protein response can be induced by a variety of stresses that take place within rapidly proliferating tumor cells, as well as in the inflammatory microenvironment. Excessive ROS generation, hypoxia, impaired calcium homeostasis, and exposure to chemotherapy are a few examples of such causes (Riaz et al., 2020). Unfolded protein accumulation in the ER promotes the oligomerization of IRE1α in membranes and IRE1α's cytosolic domain autophosphorylation. IRE1α interacts with apoptosis signal-regulating kinase-1 and TNF receptor-associated factor-2 to activate c-Jun-N-terminal kinase (JNK), a stress kinase that induces apoptosis or autophagy (Ron and Hubbard, 2008). Moreover, the transcription factor X Box-binding protein 1 (XBP-1) is regulated by the IRE1 RNAse domain and transcriptionally activates Beclin1 to cause autophagy (Margariti et al., 2013).

ATF6 is moved to the Golgi compartment after ERS, where Site-1/-2 proteases degraded it. The cleaved ATF6 then enters the nucleus and interacts with ERS-response elements and ATF/cAMP response elements to activate target genes such CHOP, XBP-1, glucose-regulated protein 78 (GRP78)/ binding immunoglobulin protein (BiP). Then, through CHOP and XBP-1, ATF6 indirectly controls apoptosis or autophagy (Adachi et al., 2008).

Autophagy and apoptosis can be triggered by an elevation in $[Ca^{2+}]i$ flow into the cytoplasm under ERS circumstances. According to Hayer-Hansen et al. (2007), the released Ca^{2+} activates protein kinase C (PKC), provokes CaMKK/AMPK-dependent pathway, inhibits mTOR, and activates death-associated protein kinase, which is involved in the phosphorylation of Beclin1 and subsequent Beclin1/Bcl-2 complex disruption. Through Ca^{2+}-mediated mitochondrial cell death, the released Ca^{2+} also stimulates apoptosis (Høyer-Hansen et al., 2007). Autophagy and apoptosis are closely

related in the upstream signal pathways (IRE1, ATF6, and Ca^{2+}) (Song et al., 2017).

It is widely known that ROS can activate the Raf/MEK/ERK signaling pathways by acting directly on growth receptors like platelet-derived growth factor receptor and epidermal growth factor receptor leading to activation of Ras and ERK1/2. Moreover, ROS trigger the activation of ERK1/2 signaling through the proto-oncogene c-Src and the inhibition of protein phosphatases. c-Src can phosphorylate and activate phospholipase C-γ, which produces diacylglycerol and raises $[Ca^{2+}]i$, that in turn triggers the activation of various types of PKC. PKC has been demonstrated to directly activate Raf and Ras (Lee and Esselman 2002; McCubrey et al., 2007).

The observed up-regulation of Raf/MEK/ERK expressions is consistent with previous studies which indicated that activation of Raf/MEK/ERK had been linked to advanced PCa, hormonal independence, as well as poor prognosis (Mukherjee et al., 2005). Some PCa may respond better to treatments that boost Raf/MEK/ERK activation because these treatments may cause senescence, cell cycle arrest, or terminal differentiation (McCubrey et al., 2007).

The current results showed that although treatment with TRA and/or KET increases the formation of ROS, which in turn impacts several cellular functions including migration, the expression of E- and N-cadherin was upregulated in most treated cancer cells. These findings are consistent with other research that suggests raising the intracellular ROS threshold may be used to treat or prevent PCa metastasis and growth as well as to block the EMT pathway (Das et al., 2014). The prevention of tumor progression to a more invasive type was also linked to increased E-cadherin expression. As a result, E-cadherin can be regarded as a tumor suppressor (Kourtidis et al., 2017). In the polarized environment of macrophages, several inflammatory molecules (TGF-β, TNF-α, and IL) could down-regulate β-catenin expression, blocking the Wnt/β-catenin pathway, then upregulate the expression of E-cadherin and prevent EMT (Chen et al., 2019).

Cadherin switching, which typically refers to a switch from E- to N-cadherin expression, also involves conditions wherein E-cadherin levels remain relatively constant but cells activate N-cadherin expression. N-cadherin is not essential for the EMT process itself, but it controls the cell's behavior after EMT including its ability for migration (Maeda et al., 2005). The cellular environment and the health of the tissue (disease state) determine whether N-cadherin acts as a promoter or an inhibitor of cell proliferation. According to Su et al., N-cadherin serves as a growth suppressor, and its absence activates the Wnt/β-catenin pathway (Su et al., 2016).

The differing invasive and proliferative characteristics of PC-3 and DU145 cells may be related to the activation of p53 gene in both cells. The p53 gene has two mutations in DU145 cells, at codons 274 and 223, while PC-3 cells have one mutation at chromosome 17p (Chappell et al., 2012). The reduced vulnerability of DU145 cells to the anticancer effects of TRA and/or KET may be caused by the fact that PC-3 cells have just one p53 mutation while DU145 cells have two p53 mutations.

Conclusion: The potential function of TRA and/or KET in PCa cell lines is supported by the upregulation of genes related to apoptosis, autophagy, necroptosis, parthanatos, ERS, Raf/MEK/ERK pathway, and EMT. The mechanism by which these medications combat metastatic PCa may be inducing ROS. This mechanism may be a desirable strategy for cancer treatment, especially for more advanced malignancies. Similar strategies might be applied effectively to other cancers.

The best strategy for creating anticancer therapies is to target cell death pathways. TRA and/or KET may be such compounds that are nontoxic to normal cells. TRA is a more effective anticancer drug than KET, as well as TRA alone, exerts a more pronounced anticancer impact than when combined with KET.

AUTHOR CONTRIBUTIONS

NH and KA: Resources, Formal analysis, Writing, Review, Editing. MA: Supervision, Review.

DATA AND MATERIALS AVAILABILITY

All data analyzed during this study are included in the article.

FUNDING

Not applicable.

CONFLICT OF INTEREST

All authors have no conflict of interest.

REFERENCES

Abdollahpour A, Saffarieh E, Zoroufchi BH (2020). A review on the recent application of ketamine in management of anesthesia, pain, and health care. J Family Med Primary Care; 9 :1317-1324.

Adachi Y, Yamamoto K, Okada T, Yoshida H, Harada A, Mori K (2008). ATF6 is a transcription factor specializing in the regulation of quality control proteins in the endoplasmic reticulum. Cell Struct Funct; 33: 75-89.

Bameri B, Shaki F, Ahangar N, Ataee R, Samadi M, Mohammadi H (2018). Evidence for the involvement of the dopaminergic system in seizure and oxidative damage induced by tramadol. Int J Toxicol; 37: 164-170.

Barakat A (2019). Revisiting tramadol: a multi-modal agent for pain management. CNS Drugs; 33: 481-501.

Belal T, Awad T, Clark CR (2009). Determination of paracetamol and tramadol hydrochloride in pharmaceutical mixture using HPLC and GC-MS. J Chromatographic Sci; 47: 849-854.

Beretta GL, Zaffaroni N (2022). Necroptosis and prostate cancer: molecular mechanisms and therapeutic potential. Cells; 11: 1221.

Chappell WH, Lehmann BD, Terrian DM, Abrams SL, Steelman LS, McCubrey JA (2012). P53 expression controls prostate cancer sensitivity to chemotherapy and the MDM2 inhibitor Nutlin-3. Cell Cycle; 11: 4579-4588 .

Chen Y, Wen H, Zhou C, Su Q, Lin Y, Xie Y, Huang Y, Qiu Q, Lin J, Huang X, Tan W (2019). TNF-α derived from M2 tumor-associated macrophages promotes epithelial–mesenchymal transition and cancer stemness through the Wnt/β-catenin pathway in SMMC-7721 hepatocellular carcinoma cells. Exp Cell Res; 378: 41-50.

Das TP, Suman S, Damodaran C (2014). Induction of reactive oxygen species generation inhibits epithelial–mesenchymal transition and promotes growth arrest in prostate cancer cells. Mol carcinog; 53: 537-547.

Dickens LS, Powley IR, Hughes MA, MacFarlane M (2012). The 'complexities' of life and death: death receptor signaling platforms. Exp Cell Res; 318: 1269-77.

Gillessen S, Attard G, Beer TM, Beltran H, Bjartell A, Bossi A, et al (2020). Management of patients with advanced prostate cancer: report of the advanced prostate cancer consensus conference 2019. Eur Urol; 77: 508-547.

Hasan A, Rizvi SF, Parveen S, Pathak N, Nazir A, Mir SS (2022). Crosstalk Between ROS and autophagy in tumorigenesis: understanding the multifaceted paradox. Frontiers in oncology; 12: 1-20.

Hetz C, Zhang K, Kaufman RJ (2020). Mechanisms, regulation, and functions of the unfolded protein response. Nat Rev Mol Cell Biol; 21: 421-438.

Høyer-Hansen M, Bastholm L, Szyniarowski P, Campanella M, Szabadkai G, Farkas T, Bianchi K, Fehrenbacher N, Elling F, Rizzuto R, Mathiasen IS, Jäättelä M (2007). Control of macroautophagy by calcium, calmodulin-dependent kinase kinase-beta, and Bcl-2. Mol Cell; 25:193-205.

Huang P, Chen G, Jin W, Mao K, Wan H, He Y (2022). Molecular mechanisms of parthanatos and its role in diverse diseases. Int J Mol Sci; 23: 7292.

Ito H, Daido S, Kanzawa T, Kondo S, Kondo Y (2005). Radiation induced autophagy is associated with LC3 and its inhibition sensitizes malignant glioma cells. Int J Oncol; 26:1401-1410.

Ito H, Unchida T, Makita K (2015). ketamine causes mitochondrial dysfunction in human-induced pluripotent stem cell-derived neurons. PLoS One; 10: e0128445.

Kourtidis A, Lu R, Pence LJ, Anastasiadis PZ (2017). A central role for cadherin signaling in cancer. Exp Cell Res; 358: 78-85.

Lec PM, Lenis AT, Golla V, Brisbane W, Shuch, Garraway IP, Reiter RE, Chamie K (2020). The role of opioids and their receptors in urological malignancy: A review. J Urol; 204: 1150 1159.

Lee K, Esselman WJ (2002). Inhibition of PTPs by H2O2 regulates the activation of distinct MAPK pathways. Free Radic Biol Med; 33: 1121-1132.

Li T, Su L, Lei Y, Liu X, Zhang Y, Liu X (2015). DDIT3 and KAT2A proteins regulate TNFRSF10A and TNFRSF10B expression in endoplasmic reticulum stress-mediated apoptosis in human lung cancer cells. J Biol Chem; 290: 11108-11118.

Maeda M, Johnson KR, Wheelock MJ (2005). Cadherin switching: essential for behavioral but not morphological changes during an epithelium-to-mesenchyme transition. J Cell Sci;118: 873-887 .

Mahmoud G, Hussein OE, Hozayen WG, Abd El-Twab SM (2017). Methotrexate hepatotoxicity is associated with oxidative stress, and down-regulation of PPAR gamma and Nrf2: protective

effect of 18beta-glycyrrhetinic acid. Chem Biol Interact; 270: 59-72.

Margariti A, Li H, Chen T, Martin D, Vizcay-Barrena G, Alam S, Karamariti E, Xiao Q, Zampetaki A, Zhang Z, Wang W, Jiang Z, Gao C, Ma B, Chen YG, Cockerill G, Hu Y, Xu Q, Zeng L (2013). XBP1 mRNA splicing triggers an autophagic response in endothelial cells through BECLIN-1 transcriptional activation. J Biol Chem; 288: 859-872.

McCubrey JA, Steelman LS, Chappell WH, Abrams SL, Wong EW, Chang F, Franklin RA (2007). Roles of the Raf/MEK/ERK pathway in cell growth, malignant transformation and drug resistance. Biochim Biophys Acta; 1773: 1263-1284.

Mendoza FJ, Ishdorj G, Hu X, Gibson SB (2008). Death receptor-4 (DR4) expression is regulated by transcription factor NF-κB in response to etoposide treatment. Apoptosis; 13: 756-770.

Mohamed HM, Mahmoud AM (2019). Chronic exposure to the opioid tramadol induces oxidative damage, inflammation and apoptosis, and alters cerebral monoamine neurotransmitters in rats. Biomed Pharmacother; 110: 239-247.

Mohanty S, Yadav P, Lakshminarayanan H, Sharma P, Vivekanandhan A, Karunagaran D (2022). RETRA induces necroptosis in cervical cancer cells through RIPK1, RIPK3, MLKL and increased ROS production. Eur J Pharmacol; 920: 174840.

Mukherjee R, Bartlett JMS, Krishna NS, Underwood MA, Edwards J (2005). Raf-1 expression may influence progression to androgen insensitive prostate cancer. Prostate; 64: 101-107.

Pazzaglia S, Pioli C (2019). Multifaceted role of PARP-1 in DNA repair and inflammation: pathological and therapeutic implications in cancer and non-Cancer diseases. Cells; 9: 41.

Redza-Dutordoir M, Averill-Bates DA (2021). Interactions between reactive oxygen species and autophagy: Special issue: Death mechanisms in cellular homeostasis. Biochim Biophys Acta Mol Cell Res; 1868: 119041.

Riaz TA, Junjappa RP, Handigund M, Ferdous J, Kim HR, Chae HJ (2020). Role of endoplasmic reticulum stress sensor IRE1alpha in cellular physiology, calcium, ROS signaling, and metaflammation. Cells; 9: 1160.

Ron D, Hubbard SR (2008). How IRE1 reacts to ER stress. Cell; 132: 24– 26.

Shen X, Xue Y, Si Y, Wang Q, Wang Z, Yuan J and Zhang X (2015). The unfolded protein response potentiates epithelial-to-mesenchymal transition (EMT) of gastric cancer cells under severe hypoxic conditions. Med Oncol; 32: 447.

Song S, Tan J, Miao Y, Li M, Zhang Q (2017). Crosstalk of autophagy and apoptosis: Involvement of the dual role of autophagy under ER stress. J cellular physiol: 232; 2977-2984.

Su Y, Li J, Shi C, Hruban RH, Radice GL (2016). N-cadherin functions as a growth suppressor in a model of K-ras-induced PanIN. Oncogene; 35: 3335-3341.

Sung H, Ferly J, Siegel RL, Laversanne M, Soerjomataram I, Jemal A, Bray F (2021). Global cancer statistics 2020: Globocan estimates of incidence and mortality worldwide for 36 cancers in 185 countries. CA Cancer J Clin; 209-249.

Valente G, Morani F, Nicotra G, Fusco N, Peracchio C, Titone R, Alabiso O, Arisio R, Katsaros D, Benedetto C, Isidoro C (2014). Expression and clinical significance of the autophagy proteins BECLIN 1 and LC3 in ovarian cancer. Biomed Res Int; 2014: 462658.

Yan G, ELBadawi M, Efferth T (2020). Multiple cell death modalities and their key features Review. W Academy Sciences J; 2: 39-48.

Zhang F, Xie R, Munoz FM, Lau SS, Monks TJ (2014). PARP-1 hyperactivation and reciprocal elevations in intracellular Ca2+ during ROS-induced nonapoptotic cell death. Toxicol Sci; 140: 118-134.

Zhang Y, SU SS, Zhao S, Yang Z, Zhoong CQ, Chen X, Cai Q, Yang ZH, Huang D, Wu R, Han J (2017). RIP1 autophosphorylation is promoted by mitochondrial ROS and is essential for RIP3 recruitment into necrosome. Nat Commun; 8: 14329.